COVER SHEET

Title: Predicting Stochastic Lightning Mechanical Damage Effects on Carbon Fiber Reinforced Polymer Matrix Composites

Authors: Juhyeong Lee
Syed Zulfiqar Hussain Shah

Paper Number: 16

(FIRST PAGE OF ARTICLE)

ABSTRACT

Three stochastic air blast models are developed with spatially varying elastic properties and failure strengths for predicting lightning mechanical damage to AS4/3506 carbon/epoxy composites subjected to < 100 kA peak currents: (1) the conventional weapon effects program (CWP) model, (2) the coupled eulerian-lagrangian (CEL) model, and (3) the smoothed-particle hydrodynamics (SPH) model. This work is an extension of our previous studies [1–4] that used deterministic air blast models for lightning mechanical damage prediction. Stochastic variations in composite material properties were generated using the Box-Muller transformation algorithm with the mean (i.e., room temperature experimental data) and their standard deviations (i.e., 10% of the mean herein as reference). The predicted dynamic responses and corresponding damage initiation prediction for composites under equivalent air blast loading were comparable for the deterministic and stochastic models. Overall, the domains with displacement, von-Mises stress, and damage initiation contours predicted in the stochastic models were somewhat sporadic and asymmetric along the fiber's local orientation and varied intermittently. This suggests the significance of local property variations in lightning mechanical damage prediction. Thus, stochastic air blast models may provide a more accurate lightning mechanical damage approximation than traditional (deterministic) air blast models. All stochastic models proposed in this work demonstrated satisfactory accuracy compared to the baseline models, but required substantial computational time due to the random material model generation/assignment process, which needs to be optimized in future work.

Juhyeong Lee, Department of Mechanical and Aerospace Engineering, Utah State University, Logan, UT 84322.

Syed Zulfiqar Hussain Shah, Department of Mechanical Engineering, Universiti Teknologi PETRONAS, 32610 Seri Iskandar, Perak Darul Ridzuan, Malaysia.

INTRODUCTION

During the last two decades, a considerable number of research has been conducted to understand complex lightning physics and lightning interactions with aerospace composites, and to design/fabricate lightweight lightning protection systems. Several researchers performed experimental and numerical investigations on lightning-induced thermo-mechanical damage to aerospace materials/structures (i.e., glass/epoxy and carbon/epoxy composites). Typical lightning damage modes in these material systems involve fiber damage (i.e., breaking, splitting, tow separation), matrix damage (i.e., cracking, thermal decomposition), and inter-/intra-ply delamination. Presently, the majority of recent lightning studies were focused on investigating the lightning damage resistance and tolerance of composite structures against different impulse current waveforms [5–8] and design configurations, such as ply orientation, stacking sequence, lightning protection layer, use of conductive filler and matrix [9–11].

Several multiphysics models were developed primarily to predict lightning thermal damage in composites since the domain of thermal damage is more clearly visible and widespread than that of mechanical damage. Researchers have paid less attention to characterizing lightning mechanical damage due to complex nature of lightning-induced mechanical loading (i.e., shock wave and electromagnetic forces) and technical challenges in isolating pure lightning damage from lightning test results. As a result, accurate lightning mechanical damage models are not yet well developed. This motivates the present study to propose novel stochastic air blast models for predicting lightning mechanical damage to aerospace composites.

Some composite material property varies locally with heterogenous microstructure together with the size. The random distribution of constituents and defects (fiber waviness or winkling, resin-rich pockets, voids, etc.) has a significant influence on the elastic constants and strength properties due to their heterogeneous nature. These defects significantly degrade the strength properties of composites, such as longitudinal tensile/compressive strength, transverse tensile/compressive strength, and interlaminar shear strength, etc. In typical unidirectional carbon/epoxy composites, void content and fibre/tow waviness vary up to 5% by weight [12] and 7.5° [13], as shown in Fig. 1. In general, these defects are randomly distributed throughout the composite, which influences local damage initiation within its microstructure, leading to spatial variations in all strength properties.

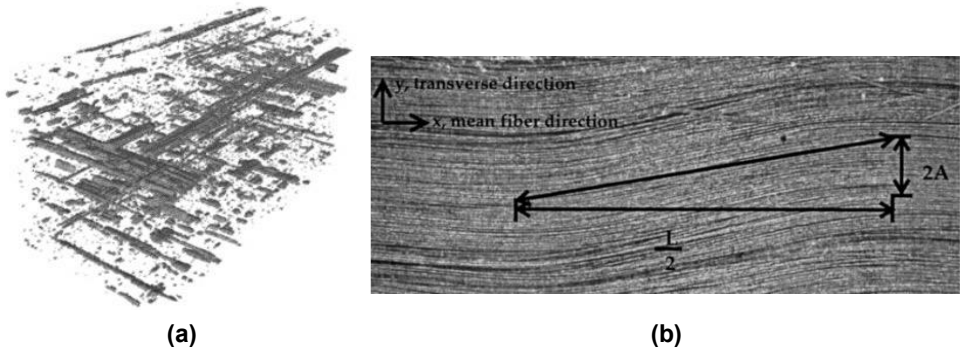

Figure 1. Micro-CT images of typical unidirectional carbon/epoxy composite: (a) 3D void distribution (~5% by weight [12]) and (b) fiber waviness (~7.5° [13]).

We propose *three* reliable and relatively simple air blast models developed with spatially varying composites' elastic properties and failure strengths for lightning mechanical damage prediction. Our recent studies [1–4] proved that equivalent air blast models established with a deterministic framework estimated mechanical damage comparable to that from plasma physics-based lightning mechanical damage models. In this work, stochastic variations in composite properties were generated using the Box-Muller (BM) transformation algorithm with the mean (experimental data) and its standard deviation (i.e., 10% of the mean herein as reference). A python code was developed to implement a stochastic model in ABAQUS/Explicit [14] that randomly selects and assigns a unique material model to each element. The effects of stochastic composite properties on mechanical damage resulting from air blast loading are mainly characterized. The dynamic responses and corresponding damage initiation in carbon/epoxy composites are estimated from each of three deterministic or stochastic air blast models. Due to similar background physics, the proposed stochastic air blast models can be easily adapted for directed energy-induced mechanical damage prediction.

TECHNICAL BACKGROUND

The Conventional Weapons Effects Program (CONWEP) [15] is a numerical implementation of the well-known empirical air blast models developed for free-air and surface bursts by Kingery and Bulmash [16]. Using a substantial set of experimental data, Kingery and Bulmash [16] proposed higher-order polynomials to approximate all air blast parameters (i.e., incident and reflected overpressures, their impulses, and shock-front velocity) defined as a function of a scaled distance – a parameter primarily characterized by the intensity of blast overpressure. According to the Hopkinson-Cranz law [17,18], the scaled distance Z (m/kg$^{1/3}$) is the stand-off distance R (m), defined as the distance from the explosion center and the target structure, divided by the cube-root of the explosive charge weight W (kg), i.e., $Z = R/W^{1/3}$. For explosives other than TNT, W can be replaced with the TNT equivalent weight (kg TNT). In general, a near-field explosion ($Z < 1.18$ m/kg$^{1/3}$) involves numerous blast wave reflections occurring simultaneously and interfering with each other. Thus, the resulting dynamic overpressure and impulse loading profiles are highly non-uniform. As a result, air blast parameters predicted by the CONWEP model for a near-field explosion are less accurate than for a far-field explosion.

The propagation and attenuation characteristics of incident and reflected blast waves are strongly influenced by the surrounding air. For instance, the viscous effects of the propagating shock-front in the surrounding air and at the structure wall significantly attenuate air blast loading, particularly for a far-field explosion, thus reducing damage to the structure. In practice, air blast loading on structure is a fluid-structure interaction (FSI) problem. The two most common numerical frameworks for characterizing interactions between the gaseous/liquid flow and the structure are (1) a coupled Eulerian-Lagrangian (CEL) model and (2) a smoothed-particle hydrodynamics (SPH) model. Each model combines the Lagrangian configuration of a fixed solid domain with the Eulerian or SPH configuration of a moving fluid domain. The major difference is that a CEL model performs Eulerian and Lagrangian

analyses simultaneously, while a SPH model is a mesh free method developed only on a Lagrangian formulation (so only Lagrangian analysis is performed). Note that the Lagrangian mesh is attached to the material and elements deform as the material deforms, while the Eulerian mesh is stationary (i.e., fixed in space) and material flows through elements without deformation [14]. The Eulerian mesh is preferable for simulating problems involving large deformation, but it requires mesh refinement, a small time increment, and intensive computational resources due to its boundary conditions [19].

In a CEL model, an explosive is modeled in an Eulerian domain and included in the surrounding area (also modeled in an Eulerian domain). The blast waves propagate from an explosive through the surrounding air and impacts the structure (modeled in a Lagrangian domain). Structural dynamics after a shock arrival time are primary areas of interest. A blast wave is followed by a cloud (or fireball) of hot gases emanating from an explosive. These hot gas mixtures resulting from the product of detonation are often characterized using an equation of state (EOS) that calculates the thermodynamic properties (pressure, volume, temperature in thermodynamic equilibrium). The JWL EOS [20] is frequently used for simulating the detonation of a high explosive (i.e., TNT), and an ideal gas EOS is used to model ambient air.

In contrast, a SPH model involves a mesh free representation of an explosive in a Lagrangian domain. Finite element conversion to SPH particles is based on time, strain, and stress-based criteria, regardless of the deformation levels. SPH particles interact with their neighboring particles through a kernel function during the analysis. The SPH formulation requires a greater number of particles and a small time increment to achieve sufficient accuracy in final results, making it computationally demanding. The number of particles per element, their initial distribution, appropriate kernel function, and an efficient particle search routine within a SPH domain must be well defined to improve model accuracy and numerical stability.

FINITE ELEMENT MODELS

The present study is an extension of our earlier work [1–4] that proposed a deterministic finite element (FE) modeling framework for lightning damage prediction in carbon/epoxy composites. Using the deterministic models as a baseline, we primarily incorporated the stochastic nature of elastic properties and failure strengths, allowing us to predict asymmetric lightning damage in composites, which will be more consistent with physical observation. The baseline (deterministic) CONWEP, CEL, and SPH models are briefly discussed in this paper; more technical details and theoretical background on each model can be found in Refs. [1–4]. The stochastic modeling framework developed in this paper is also described in the following section.

Baseline Lightning Mechanical Damage Models

All baseline models were developed for a 16-ply quasi-isotropic, $[45/0/–45/90]_{2S}$, laminate consisting of 0.29-mm-thick unidirectional AS4/3506 carbon/epoxy plies subjected to simulated 40, 50, and 100 kA peak currents. The scaled distance Z and the weight of TNT explosive charge W were calculated for equivalent air blast models. TABLE I summarizes all air blast parameters used to develop the FE models.

TABLE I. AIR BLAST MODEL PARAMETERS.

Peak current (kA)	TNT Charge W (g)	Scaled Distance[1] Z (m/kg$^{1/3}$)	TNT Radius[2] (mm)
40	0.16	0.183	2.9
50	0.20	0.170	3.1
100	0.41	0.135	3.9

[1]Similar to our previous work [2], Z is determined by assuming the stand-off distance R = 0.01.
[2]Assuming a spherical TNT explosive, the radius was calculated with its density (1654 kg/m^3).

In all CONWEP, CEL, and SPH models, the carbon/epoxy laminates with in-plane dimensions of 150 × 150 mm^2 were modeled in a Lagragian domain using four-node shell elements with reduced integration and a large-strain formulation (S4R elements [14]) with a global size of 2 mm; all four edges of the laminates were encastred (i.e., U1 = U2 = U3 = UR1 = UR2 = UR3 = 0) during the simulations; laminate failure due to equivalent air blast loading was predicted using ABAQUS built-in Hashin failure criteria [14]. Note that the CONWEP model (Fig. 1a) involves the laminate only, thus no FSI is considered. In the CEL model (Fig. 1b), the 150 × 150× 150 mm^3 air domain was modelled for the surrounding air and discretized using Eulerian elements with a global size of 5 mm. The volumes and radii of spherical (assumed) TNT charges were calculated from the weight of TNT charges with their density 1654 kg/m^3. The volume of a TNT explosive is proportional to a peak lightning current and can be determined from equivalent chemical potential energy, according to the method proposed in [2]. In the CEL model, the TNT explosive was discretized with 0.5 mm Eulerian elements and located at a scaled distance from the composite center. The SPH model (Fig. 1c) includes the TNT explosive discretized using 8-node linear brick elements (C3D8R elements [14]) with a global size of 0.5 mm. In an SPH formulation, a cubic spline kernel function was used for the smoothing function and one particle was generated per element as the analysis started (time-based conversion, t = 0). The surrounding air was not simulated in present study due to high computational burden associated with SPH particle interactions. TABLE II provides details on the mesh statistics for each model including the number and size of elements in the mesh.

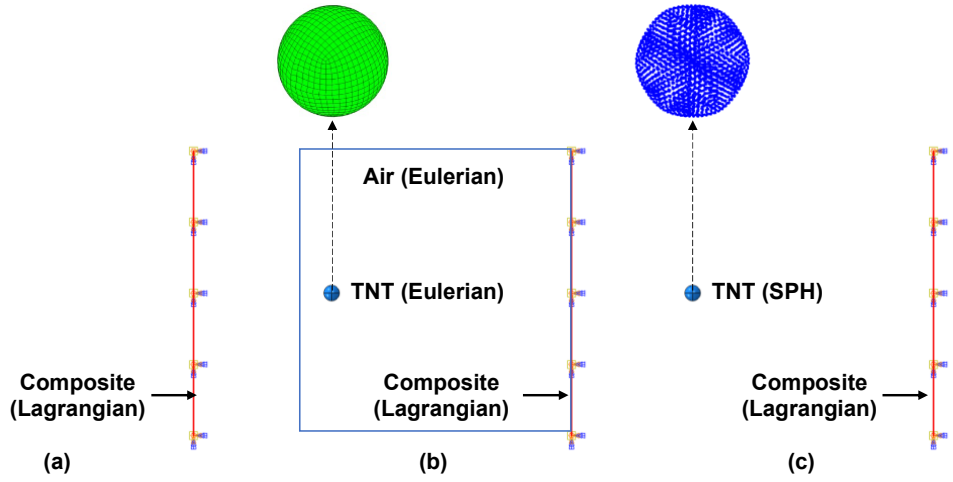

Figure 2. FE representation of each air blast model: (a) CWP, (b) CEL, and (c) SPH models.

TABLE II. MESH STATISTICS FOR BASELINE MODELS.

Model	Part	Finite Element			
		Type	Global Size[1]	Total number	
CWP	Laminate	Lagrangian	2 mm	5,776	5,776
CEL	Air	Eulerian	5 mm	36,000	43,096
	TNT	Eulerian	0.5 mm	1,320	
	Laminate	Lagrangian	2 mm	5,776	
SPH	TNT/SPH[2]	Lagrangian	0.5 mm	1,320	7,096
	Laminate	Lagrangian	2 mm	5,776	

[1]Approxmiate global element size with the default curvature control and minimum size control.
[2]The element to particle conversion ratio = 1.

Stochastic Modeling Framework

A python code is used to implement a stochastic model in Abaqus that randomly selects and assigns unique material model to each ply of the element. Figure 2 depicts the proposed algorithm's pseudo-code, which produces random elastic properties and failure strengths, and assigns them to each ply of the FE model. The code requires a pre-defined number of elements (n), number of plies (p), mean (μ) and standard deviation (σ) of strength properties as an input. The BM transformation [21] is used to generate a pair of two independent random variables (Z_1 and Z_2) with a standard normal distribution using two random numbers (R_1 and R_2). These random numbers are generated using a uniform distribution on a unit interval [0, 1].

$$\begin{aligned} Z_1(0,1) &= \cos(2\pi R_1)\sqrt{-2ln(R_2)} \\ Z_2(0,1) &= \sin(2\pi R_1)\sqrt{-2ln(R_2)} \end{aligned} \tag{1}$$

These uniformly distributed random variables (Z_1 and Z_2) are then scaled based on the mean (μ) and standard deviation (σ) of strength properties in a specific range, i.e.,

$$X_{ij,n}^{k}(\mu,\sigma) = \begin{Bmatrix} \mu_{ij} + \sigma_{ij} \times Z_1(0,1) \\ \mu_{ij} + \sigma_{ij} \times Z_2(0,1) \end{Bmatrix} \tag{2}$$

where $X_{ij,n}^{k}$ represents two randomly generated elastic properties or failure strengths in two principal directions (i.e., $X_{11,n}^{T}$, $X_{11,n}^{C}$, $X_{22,n}^{T}$, $X_{22,n}^{C}$ and $X_{12,n}^{S}$). The python code randomly selects one of the two $X_{ij,n}^{k}$ and assign it to p^{th} ply of the n^{th} element in the model.

The pseudo-code (Fig. 2) may provide negative material properties (i.e., $X_{ij,n}^{k} < 0$), especially if the standard deviation is sufficiently large relative to the mean. Negative material properties may cause convergence problems during FE simulation. To avoid this situation, the code re-generates material properties until it returns positive values. After a complete set of positive, random material properties were generated, a material model "MAT-n" is defined and assign it to p^{th} ply of the nth element in the model. This process is repeated until random material properties were assigned to all the plies of the FE model. Figure 3 compares the FE meshes generated in the deterministic and stochastic models, where each color represents a FE with a unique material model. As stated earlier, this work considered stochastic

variations in composite's elastic properties and failure strengths. All stochastic composite properties were generated with mean the (experimental data) and its standard deviation (i.e., 10% of the mean herein as reference). TABLE III includes AS4/3506 carbon/epoxy lamina properties used in present FE models.

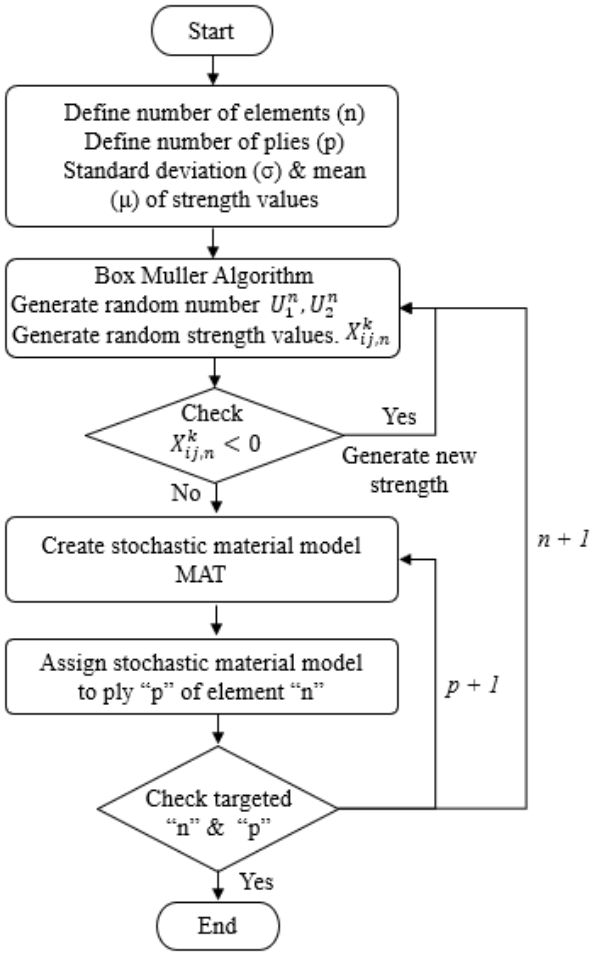

Figure 3. Schematic flowchart of stochastic material model generation and assignment.

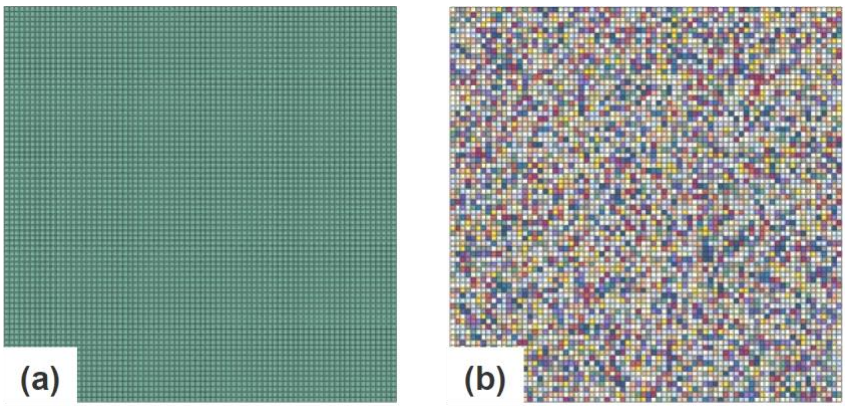

Figure 4. FE meshes generated within (a) deterministic and (b) stochastic frameworks.

TABLE III. AS4/3506 CARBON/EPOXY LAMINA PROPERTIES [22,23] USED IN THE STOCHASTIC FE MODELS.

Elastic Properties[1]	E_{11} (GPa)	$E_{22} = E_{33}$ (GPa)	$G_{12} = G_{13}$ (GPa)	G_{23} (GPa)	$\nu_{12} = \nu_{13}$	ν_{23}
μ	142.50	9.80	6.28	3.75	0.29	0.30
σ	14.25	0.98	0.63	0.38	0.03	0.03
Failure Strengths[2]	X_T (MPa)	X_C (MPa)	Y_T (MPa)	Y_C (MPa)	S_L (MPa)	S_T (MPa)
μ	2280	1440	57	228	71	71
σ	228	144	5.7	22.8	7.1	7.1

[1]E_{11}, E_{22}, and E_{33} are elastic moduli in the longitudinal (1), transverse (2), and through-thickness (3) directions, respectively; G_{12}, G_{13}, and G_{23} are shear moduli in the 1–2, 1–3, 2–3 planes, respectively.
[2]X_T/X_C are longitudinal tensile/compressive strength; Y_T/Y_C are transverse tensile/compressive strength; S_L/S_T are longitudinal/transverse shear strength.

RESULTS AND DISCUSSION

Computational time is an important metric to evaluate the performance of numerical simulations. Figure 4 compares the total computational time required to complete all blast models. Herein, the total computational time includes (1) the time required for stochastic material model generation/assignment and (2) the CPU time to solve the problems, for all deterministic and stochastic air blast models. In the figure, the labels *E* and *S* represent stochastic models with random elastic properties and random failure strengths, respectively. As expected, all stochastic models required a considerable amount of computational time compared to the baseline (deterministic) models. This is primarily associated with stochastic material model generation and assignment. The random material model generation code (Fig. 2) (1) produces a unique material property set, (2) creates a section, and (3) assigns the section to each finite element. It is expected that as the number of elements in the mesh increases, the time required to create corresponding random material models exponentially increases, while the accuracy of the solution improves. Note that the algorithm (Fig. 2) proposed for stochastic material model generation in this study is proof-of-concept and has not been optimized yet. The algorithm is currently optimized to reduce the total computational time. The CPU times for all models were indeed similar to each other, regardless of the modeling framework. Overall, the CONWEP models were computationally efficient as they required a smaller number of elements (TABLE II) due to no FSI, compared to the CEL and SPH models.

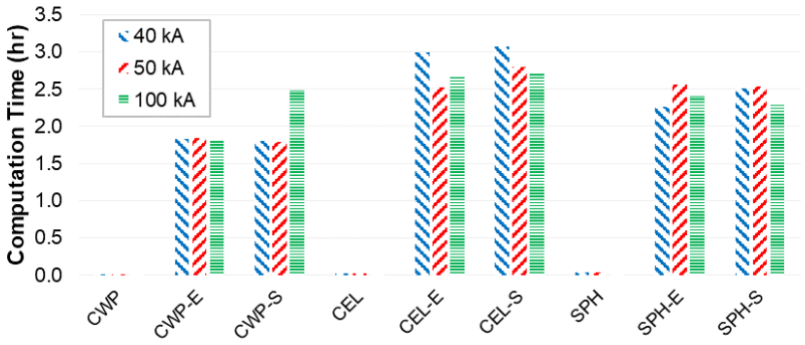

Figure 5. Total computational time required to complete all deterministic and stochastic models.

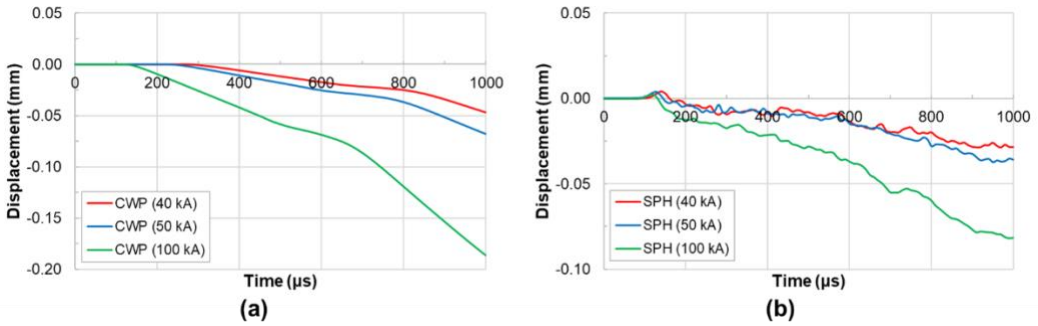

Figure 6. Temporal variations in the transverse displacements captured at the laminate's geometric center using: (a) CWP models and (b) SPH models.

In all air blast models, a TNT explosive was located at the scaled distance (*Z* in TABLE I) away from the laminate center. A blast wave arrival time (i.e., the time required for air blast waves to propagate from the explosion center to the laminate) varies with a scaled distance *Z*, i.e., a smaller *Z* (representing greater lightning peak current) from the laminate results in a faster blast wave arrival time. For accurate model validation and subsequent calibration purposes, it is important to evaluate all the dynamic responses of laminate at the same time after the blast wave arrives. Figure 6 compares the time evolution of transverse mid-plane displacements predicted at the composite's geometric center using the CONWEP and SPH models. A blast wave arrival time was roughly in the range of 150 ~300 μs for the CONWEP models and <100 μs for the SPH models. The CONWEP models showed a considerable delay in the blast arrival time for a larger scaled distance (40 kA), while the results in the SPH models were insensitive to a scaled distance (corresponding to peak current). Therefore, we generated all results with zero arrival times in the following section. This post-processing allows to capture dynamic responses at the same time-scale after the incident wave reaches the laminate.

Figure 7 shows the transverse displacements and strain-rates captured at the AS4/3506 carbon/epoxy laminate's geometric center predicted using the baseline and stochastic air blast models consistent with 40, 50, and 100 kA peak currents. The resulting dynamic responses were comparable for each baseline and stochastic model. As shown in the three left subfigures of Fig. 7, air blast loading led to somewhat monotonic compressive deformation by 500 μs. The predicted peak compressive displacements gradually increased as the peak current amplitude increased from 40 to 100 kA; these were roughly in the range of -0.02 ~ -0.07 mm (for the CONWEP models, Fig. 7a), -0.03 ~ -0.1 mm (for the CEL models, Fig. 7c), and -0.01 ~ -0.03 mm (for the SPH models, Fig. 7e). As expected, the results from the baseline models and stochastic models with varying failure strengths (i.e., CWP-S, CEL-S, and SPH-S) were overlapped. This makes sense since the laminate's elastic properties defined in the models are the same, thus their dynamic responses (prior to damage initiation) must be identical as well. The predicted strain-rates at the laminate center were also comparable for the CONWEP models (Fig. 7b) and CEL models (Fig. 7d). In contrast, the SPH models (Fig. 7f) predicted a large degree of fluctuation between tensile and compressive strain-rates, presenting severe SPH particle-to-particle interactions and collisions at the end of each time increment during the simulations.

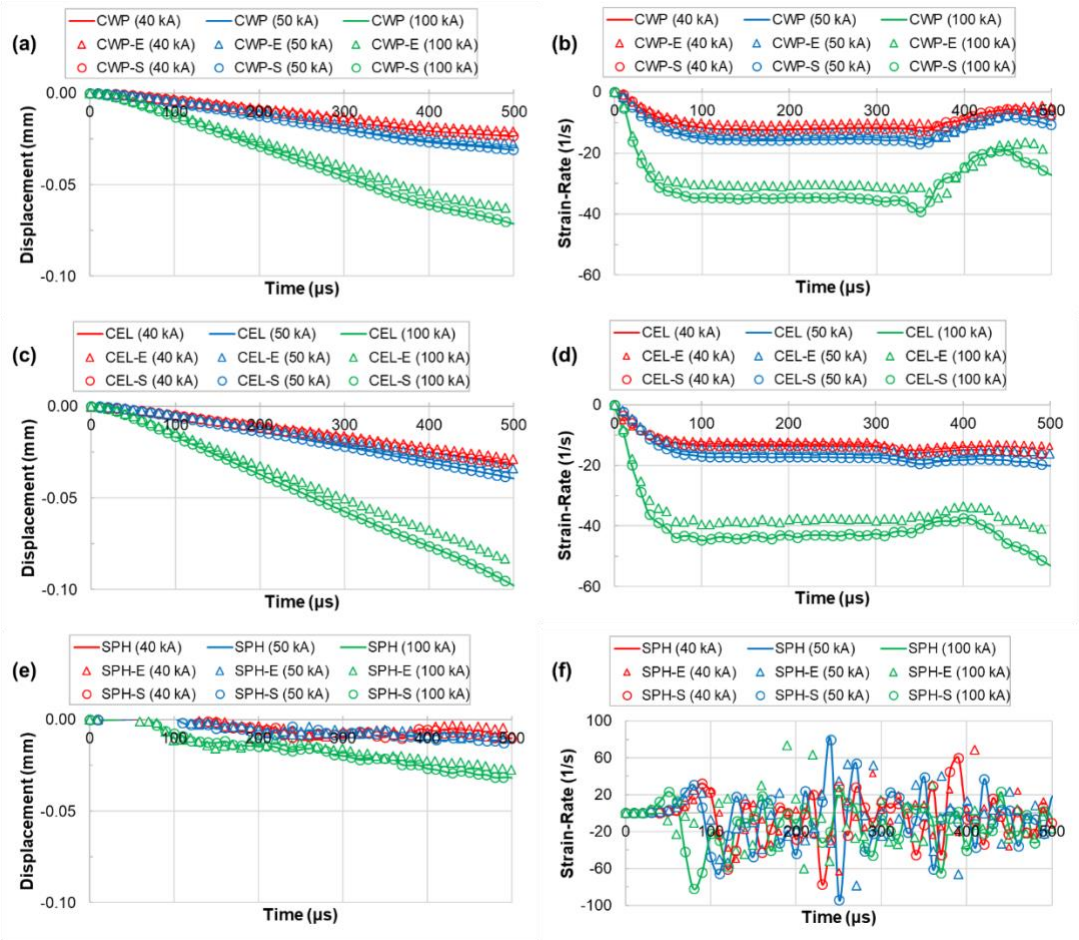

Figure 7. Transverse displacements (left) and corresponding strain-rates (right) at the composite's geometric center predicted using: (a)-(b) CONWEP, (c)-(d) CEL, and (e)-(f) SPH models.

Displacement magnitude contours predicted at the laminate's outermost (impacted) ply from 100 kA peak current are compared in Fig. 7. The key results from the figure can be summarized as follows: (1) the predicted shape, size, and magnitude of the domain with displacement magnitude contours estimated by the deterministic and stochastic damage models were similar to each other; (2) the results from the CONWEP models showed good agreement with those from the CEL models; (3) the SPH displacement contours were asymmetric, and their magnitudes were relatively small. Although not included in this work, the overall domains of interest (i.e., highlighted in the Fig. 7) and the peak displacement magnitude increased substantially with increasing peak lightning current.

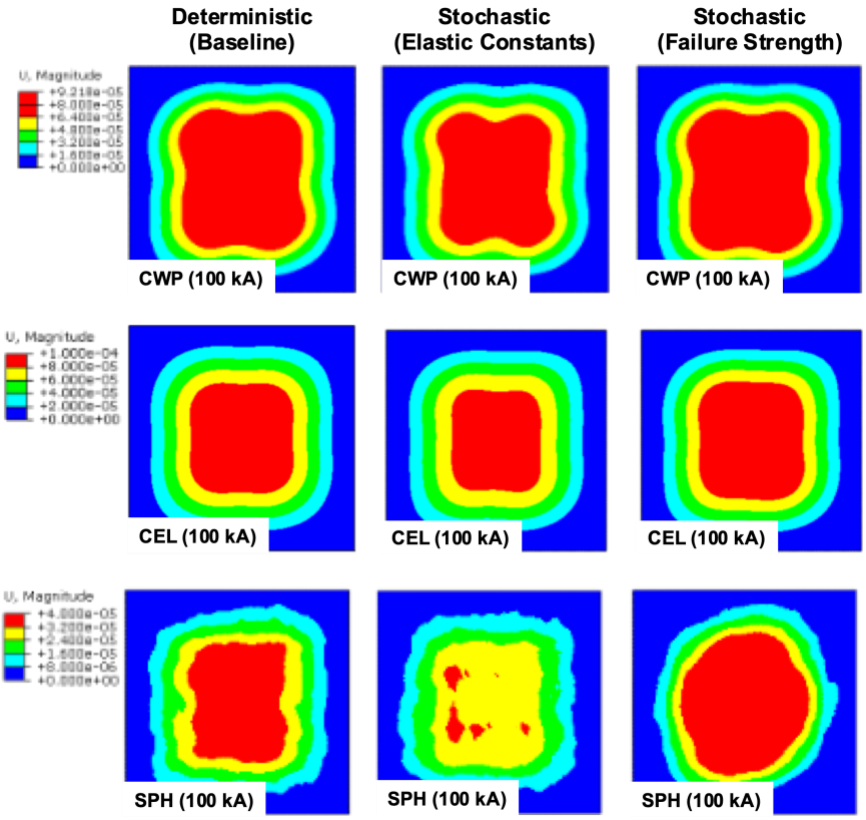

Figure 8. Displacement magnitude contours on the outermost composite ply at 500 μs from 100 kA.

The corresponding von-Mises (VM) stress contours on the outermost composite ply for 100 kA peak current are compared in Fig. 8. In the CONWEP and CEL models, the magnitudes and locations of the maximum VM stress predicted from the deterministic models were coherent with those from the stochastic models. For instance, the CONWEP models estimated the maximum VM stress at the middle of (encastred) laminate's top and bottom edges, similar to the CEL models. Furthermore, both the deterministic and stochastic CONWEP models clearly identified four internal regions with local stress concentration (red in three upper subfigures of Fig. 8). Two important findings from the VM stress contours are: (1) smoothness of contour lines and (2) patterned versus sporadic distribution. The VM stress contours from the deterministic models were smooth, continuous vector lines, while those from the stochastic models were piecewise-smooth, but not necessarily continuous across the composite ply. The intensity of air blast loading is maximum at the laminate center and exponentially decreases as the distance from the center increases. However, the VM contours shown in Fig.°8 did not follow this trend. In practice, the laminate, once struck by air blast waves, likely experiences transient in-plane and flexural vibrations due to local stress wave transmission and reflection, leading to spatially varying stress fields. In the SPH model, air blast loading is simulated by the physical impact of SPH particles that can be interact and collide each other during the simulations. This complex SPH particle behavior is responsible for a small degree of widespread stress contours, as shown in the bottom three figures of Fig. 8). But the overall VM stress contours from the SPH models match roughly with those from the CONWEP and CEL models.

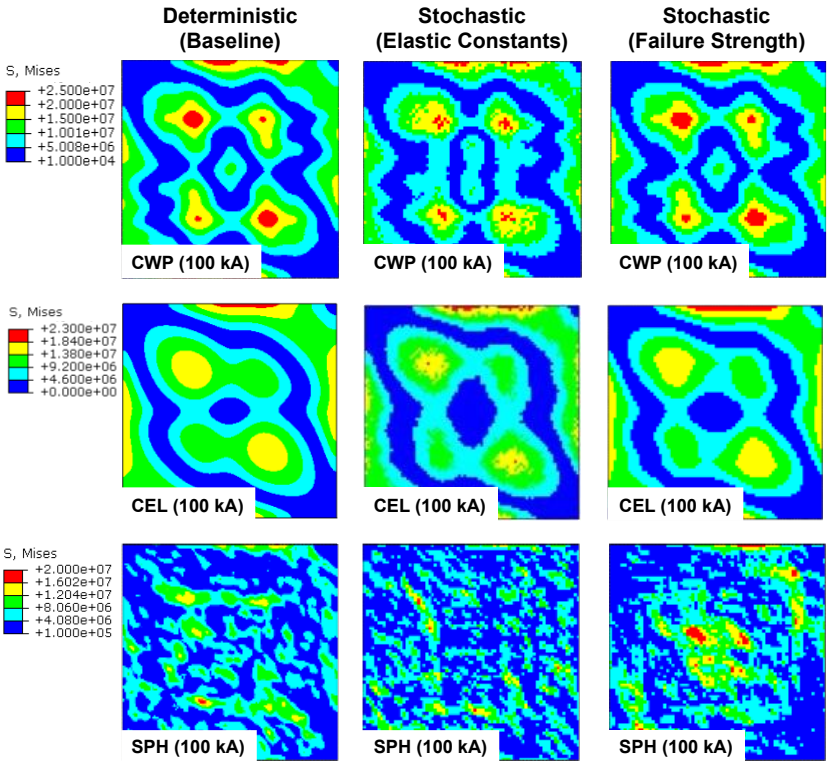

Figure 9. Von-Mises stress contours on the outermost composite ply at 500 μs from 100 kA.

This work employed the Hashin failure criteria [24,25] to approximate dynamic damage initiation of carbon/epoxy composites subjected to air blast loadings equivalent to 40, 50, and 100 kA peak currents. The Hashin criteria consider stress interactions responsible for fiber and matrix damage and is capable of predicting four mutually interacting damage initiation modes. An effective stress tensor is calculated as a function of fiber, matrix, and shear damage variables to evaluate fiber and matrix damage initiation under given loading conditions.

Similar to the VM stress contours (Fig. 8), the contours of all damage initiation indices (i.e., fiber and matrix damage in either tension or compression) varied smoothly in the deterministic models, while somewhat intermittently in the stochastic models. Figures 9 and 10 show the predicted matrix tension failure index distributions due to air blast loading associated with 50 and 100 kA peak currents, respectively. Although not included in this work, the distributions of Hashin's three other failure indices were also comparable, but their maximum magnitudes were much lower. This demonstrates that the matrix tension damage is the most significant failure mode if it occurs (i.e., failure index ≥ 1). As can be seen in the figures, the predicted matrix tension failure distributions in the outermost carbon/epoxy lamina were somewhat discrete in the stochastic models. This indicates that a significant effect of stochastic elastic properties and failure strengths on damage initiation prediction. Similar to Fig. 8, the overall domains with matrix tension damage indices were coherent for the CONWEP and CEL models. However, those predicted by the SPH models were highly sporadic (and somewhat repeated) because of local varying SPH particle-to-particle interactions and collisions. Overall, the matrix tensile damage failure indices increased slightly, but were still far less than 1.0, suggesting no mechanical damage due to < 100 kA peak currents, as consistent with our earlier work [1–4].

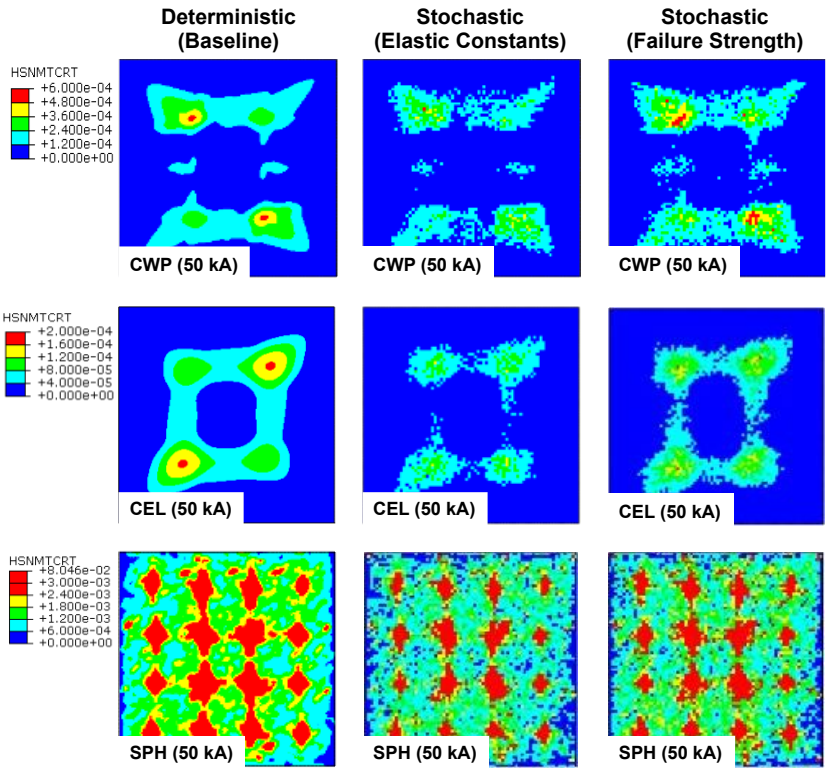

Figure 10. Hashin matrix tensile failure index distributions on the outermost composite ply at 500 μs from 50 kA.

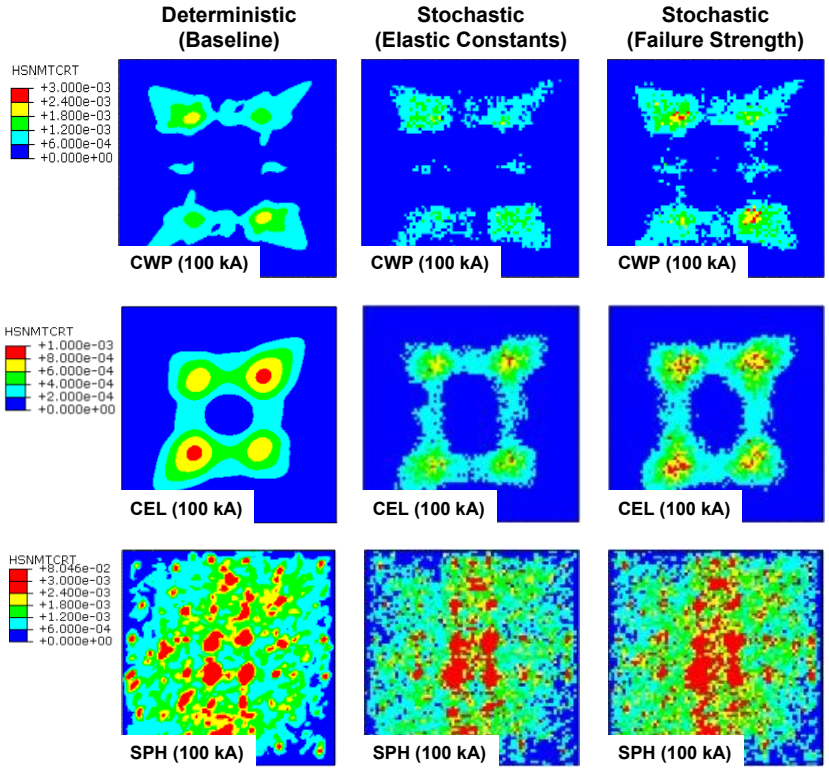

Figure 11. Hashin matrix tensile failure index distributions on the outermost composite ply at 500 μs from 100 kA.

CONCLUSION

Three stochastic air blast models were developed for predicting lightning mechanical damage in carbon/epoxy composites subjected to < 100 kA peak currents. This work is an extension of our previous studies predicting lightning mechanical damage using equivalent, deterministic air blast models. Using the Box-Muller (BM) transformation, two stochastic material models were generated: (1) elastic properties and (2) failure strengths of carbon/epoxy composites. The predicted dynamic responses and corresponding damage modes (predicted by Hashin criteria) of the laminates due to equivalent air blast loading were fairly consistent for all deterministic and stochastic models. This demonstrates that the proposed stochastic air blast models for predicting lightning mechanical damage are satisfactory and reliable. However, the stochastic models required a large computational time, primarily due to random material model generation and assignment, although the CPU times were indeed similar to the deterministic models. Note that the algorithm for stochastic material model generation proposed in this work is proof-of-concept. Thus, future work is required to optimize this algorithm.

ACKNOWLEDGEMENT

This work was partially supported by New Faculty Research Start-up Funding from the USU Office of Research.

REFERENCES

[1] Lee J, Lacy TE, Pittman Jr. CU, and Reddy JN. 2019. "Numerical Estimations of Lightning-Induced Mechanical Damage in Carbon/Epoxy Composites using Shock Wave Overpressure and Equivalent Air Blast Overpressure," *Composite Structures*, 224:111039.

[2] Lee J, Lacy TE, and Pittman CU. 2021. "Lightning Mechanical Damage Prediction in Carbon/Epoxy Laminates using Equivalent Air Blast Overpressure," *Composites Part B: Engineering*, 212:108649.

[3] Lee J, Lacy TE, and Pittman CU. 2021. "Coupled Thermal Electrical and Mechanical Lightning Damage Predictions to Carbon/Epoxy Composites During Arc Channel Shape Expansion," *Composite Structures* 255:112912.

[4] Lee J, Yang B, and Fu K. 2022. "Exploring Alternative Methods for Simulating Lightning Mechanical Damage Effects on Carbon/Epoxy Laminates," *ASME International Mechanical Engineering Congress and Exposition, Proceedings (IMECE)*, October 30-November 3, Columbus, OH, USA.

[5] Hirano Y, Katsumata S, Iwahori Y, and Todoroki A. 2010. "Artificial Lightning Testing on Graphite/Epoxy Composite Laminate," *Composites Part A: Applied Science and Manufacturing*, 41:1461–70.

[6] Feraboli P and Kawakami H. 2010, "Damage of Carbon/Epoxy Composite Plates Subjected to Mechanical Impact and Simulated Lightning," *Journal of Aircraft*, 47:999–1012.

[7] Lee J, Gharghabi P, Boushab D, Ricks T, Lacy TE, Pittman Jr. CU, Mazzola, MS, and Velicki A. 2018. "Artificial Lightning Strike Tests on PRSEUS Panels," *Composites Part B: Engineering*, 154:467–77.

[8] Boushab D, Gharghabi P, Lee J, Lacy TE, Pittman CU, Mazzola MS and Velicki A. 2021. "Lightning Arc Channel Effects on Surface Damage Development on a PRSEUS Composite Panel: An Experimental Study," *Composites Part B: Engineering*, 224:109217.

[9] Gou J, Tang Y, Liang F, Zhao Z, Firsich D, and Fielding J. 2010. “Carbon Nanofiber Paper for Lightning Strike Protection of Composite Materials,” *Composites Part B: Engineering*, 41:192–8.

[10] Lee J, Lacy TE, Pittman Jr. CU, and Mazzola MS. 2017. “Thermal Response of Carbon Fiber Epoxy Laminates with Metallic and Nonmetallic Protection Layers to Simulated Lightning Currents,” *Polymer Composites*, 39:2149–66.

[11] Kumar V, Sharma S, Pathak A, Singh BP, Dhakate SR, Yokozeki T, Okada T and Ogasawara T. 2019. “Interleaved MWCNT Buckypaper between CFRP Laminates to Improve Through-Thickness Electrical Conductivity and Reducing Lightning Strike Damage,” *Composite Structures*, 210:581–9.

[12] Little JE, Yuan X, and Jones MI. 2012. “Characterisation of Voids in Fibre Reinforced Composite Materials,” *NDT&E International*, 46:122–7.

[13] Kugler D and Moon TJ. 2002. “Identification of the Most Significant Processing Parameters on the Development of Fiber Waviness in Thin Laminates,” *Journal of Composite Materials*, 36:1451–79.

[14] Dassault Systèmes Simulia Corp. 2014. “ABAQUS Documentation”

[15] Hyde DW. 1991. “CONWEP: Conventional Weapons Effects Program,” *U.S. Army Engineer Research and Development Center (ERDC)*, Vicksburg, MS, USA.

[16] Kingery CN and Bulmash G. 1984. “Air Blast Parameters from TNT Spherical Air Burst and Hemispherical Surface Burst (ARBRL-TR-02555), *US Army Armament and Development Center - Ballistic Research Laboratory*, Aberdeen Proving Ground, MD, USA.

[17] Hopkinson B. 1915. “British Ordnance Board Minutes (13565),” *The National Archives*, Kew, London, UK.

[18] Cranz C. 1926. “Lehrbuch der ballisti,” *Рипол Классик*.

[19] Bi Z. 2018. “Finite Element Analysis Applications: a Systematic and Practical Approach,” *Academic Press*.

[20] Lee E, Finger M, and Collins W. 1973. “JWL Equation of State Coefficients for High Explosives (UCID-16189).” *Lawrence Livermore National Laboratory*, Livermore, CA, USA.

[21] Box GEP and Muller ME. 1958. “A Note on the Generation of Random Normal Deviates,” *The Annals of Mathematical Statistics*, 29:610–1.

[22] Michopoulos JG, Hermanson JG, Lliopoulos A, Lambrakos S, and Furukawa T. 2011. “On the Constitutive Response Characterization for Composite Materials Via Data-Driven Design Optimization,” *In the Proceedings of the ASME 2011 International Design Engineering Technical Conference & Computers and Information in Engineering Conference*, August 29-31, Washington, DC, USA.

[23] Daniel IM and Ishai O. 2006. “Engineering Mechanics of Composite Materials,” *Oxford University Press*.

[24] Hashin Z and Rotem A. 1973. “A Fatigue Failure Criterion for Fiber Reinforced Materials,” *Journal of Composite Materials*, 7:448–64.

[25] Hashin Z. 1980 “Failure Criteria for Unidirectional Fiber Composites,” *Journal of Applied Mechanics*, 47:329–34.